Hydrogen Production from Methane Reforming Reactions over Ni/MgO Catalyst

Wen-Sheng Dong,† Hyun-Seog Roh, Zhong-Wen Liu, Ki-Won Jun, and Sang-Eon Park*

Catalysis Center for Molecular Engineering, Korea Research Institute of Chemical Technology, P.O. Box 107, Yuseong, Daejeon 305-600, Korea
Received August 11, 2001

The catalyst Ni/MgO (Ni : 15 wt%) has been applied to methane reforming reactions, such as steam reforming of methane (SRM), partial oxidation of methane (POM), and oxy-steam reforming of methane (OSRM). It showed high activity and good stability in all the reforming reactions. Especially, it exhibited stable catalytic performance even in stoichiometric SRM ($H_2O/CH_4 = 1$). From TPR and H_2 pulse chemisorption results, a strong interaction between NiO and MgO results in a high dispersion of Ni crystallite. Pulse reaction results revealed that both CH_4 and O_2 are activated on the surface of metallic Ni over the catalyst, and then surface carbon species react with adsorbed oxygen to produce CO.

Keywords : Hydrogen, Methane reforming, Ni/MgO.

Introduction

The conversion of methane to valuable chemicals is very important. In the past decades, efforts have been made for the direct conversion of methane *via* the oxidative coupling of methane to ethane and ethylene or oxygenation to methanol and formaldehyde.[1-3] Unfortunately, so far these direct processes have not been commercialized because of very low yields of target products. A conventional route for methane conversion is to convert it into synthesis gas, which is then further converted to either methanol or higher hydrocarbons.

The dominant commercial process used to produce synthesis gas is the steam reforming of methane (SRM), and Ni/$MgAl_2O_4$ has been used as a steam reforming catalyst.[4] However, this process is highly energy intensive because the reaction is highly endothermic and a great amount of energy is consumed to vaporize excess water and heat it up to the reaction temperature. Moreover, it produces synthesis gas with a high H_2/CO ratio (>3) due to the side water gas shift (WGS) reaction, resulting in low selectivity and yield to CO. As an alternative, catalytic partial oxidation of methane (POM) is considered more promising due to the mild exothermicity, high conversion, high selectivity, suitable H_2/CO ratio (H_2/CO=2) for the Fischer-Tropsch and methanol synthesis, and the very short residence time compared with the conventional highly endothermic SRM process.[5-7] POM has been studied over numerous supported metal catalysts, such as Ni-based catalysts,[8-11] the pyrochlore and perovskite oxides containing noble metals, as well as supported noble metal catalysts.[5,12-15] Among the catalysts, Ni/MgO has been considered as a fairly good catalyst for POM.[6] However, POM has several problems, including explosion dangers and deactivation of the catalyst. Oxy-steam reforming of methane (OSRM) could be an attractive alternative. By co-feeding steam and oxygen, one can avoid explosion dangers in POM, lessen additional steam cost in SRM, shorten start-up time, and control the H_2/CO ratio by changing the feeding composition of steam, oxygen and methane. Furthermore, enhanced CH_4 conversion and H_2 yield by combination of these two reforming reactions can be obtained. Besides these advantages, the coupled process can be made mildly exothermic, nearly thermoneutral, or mildly endothermic by manipulating the process conditions. Thus, the process can be conducted in a most energy efficient and safe manner compared with SRM and POM.[16-20]

To fit the demand of the combined process of POM and SRM, finding a catalyst having good activity, selectivity and stability for all the POM, SRM and OSRM processes is necessary. In the present study, the performances of Ni/MgO for POM, SRM, and OSRM were investigated. The pulse reaction of CH_4, O_2 and CH_4/O_2 were studied to survey the detailed reaction performances of the catalyst and some mechanistic aspects.

Experimental Section

Catalyst Preparation and Characteristics. Support materials employed in this study were MgO (98%, Aldrich) and $MgAl_2O_4$. Supported Ni (15 wt%) catalysts were prepared by the molten-salt method as described elsewhere.[20-22] The BET specific surface area and pore volume of the sample were measured by nitrogen adsorption at 77 K (Micromeritics, ASAP-2400). TPR was carried out in a conventional apparatus using 5% H_2/N_2 gas with a heating rate of 10 °C/min. X-ray photoelectron spectroscopy (XPS) measurements were performed at room temperature on a VG ESCALAB 210 spectrometer, with Al Kα radiation generated at 300 watts. The analyses were operated at pass energy of 20 eV and a step size of 0.1 eV. Pulse chemisorptions were performed in a multifunction apparatus.[20] The metal dispersion, surface area and average crystallite diameter were calculated based on the methods described in reference[23] by assuming the adsorption stoichiometry of one

*To whom all correspondence should be addressed. e-mail: separk@krict.re.kr.
†Permanent address: Institute of Coal Chemistry, Chinese Academy of Sciences, Taiyuan 030001, P.R. China

hydrogen atom per nickel surface atom ($H/Ni_s = 1$).

Catalytic Reaction. Activity tests were carried out under atmospheric pressure in a fixed-bed micro-reactor. 50 mg catalysts were loaded into a quartz reactor with about a 4-mm inside diameter. The reaction temperature was measured and controlled by a thermocouple inserted directly into the top layer of the catalyst bed. Before each reaction test, the catalysts were reduced in 5% H_2/N_2 at 973 K for 3 h. The effluents from the reactor were analyzed on line by a gas chromatograph, using a fused silica capillary column.

Pulse Reaction. Pulse experiments using CH_4, O_2 and CH_4/O_2 mixed gas ($CH_4/O_2 = 2$) were performed in a quartz micro-reactor with an inner diameter of 4 mm. Before the reaction, 15 mg of each catalyst was loaded in the reactor and reduced *in situ* in 5% H_2/N_2 at 700 °C for 3 h. After that, the sample was heated to 800 °C in He (30 mL/min), and held at 800 °C for 90 min to remove any residual gases in the system, and then it was exposed to pulses of CH_4, O_2 or CH_4/O_2 (1 mL pulse, 10-15 min interval). During each pulse, the exit gases were analyzed on-line by a gas chromatograph (Shimadzu GC-8A) equipped with TCD (carbosphere column, 80 °C; helium as carrier gas). The conversion and selectivity were calculated on the basis of 100% carbon and oxygen balances. In the pulse study, CO, CO_2, CO*, and CO_2* selectivities were defined according to the following equations:

CO selectivity (%)
= (moles of CO formed/moles of CH_4 converted) × 100%
CO_2 selectivity (%)
= (moles of CO_2 formed/moles of CH_4 converted) × 100%
CO* selectivity (%)
= (0.5 × moles of CO formed/moles of O_2 converted) × 100%
CO_2* selectivity (%)
= (moles of CO_2 formed/moles of O_2 converted) × 100%

Results and Discussion

Characterization. Table 1 summarizes the BET surface area, H_2 uptake, metallic Ni dispersion, surface area of Ni, and the average crystallite diameter of Ni. The dispersion data indicate that Ni particles were rather well dispersed on $MgAl_2O_4$ and MgO. The H_2 uptake of Ni/MgO catalyst determined by H_2 pulse chemisorption was 8.72 μmol/g_{cat}. The metallic Ni dispersion, Ni surface area and average crystallite diameter of Ni calculated from H_2 uptake were 1.68%, 0.71 m^2/g, and 58 nm, respectively. Pore volume and average pore diameter of Ni/MgO were 0.120 mL/g, and 30.6 nm, respectively.

The XPS binding energy (BE) of Ni $2p_{3/2}$ electrons is 856.7 eV, which is +2.3 eV higher than that of either Ni/Al_2O_3 or Ni/CeO_2, having little interaction between Ni and supports.[20] It is well known that Ni/MgO forms solid solution, thereby resulting in a very strong interaction between NiO and MgO. Surface Ni concentration of Ni/MgO was 18.0 wt%.

The TPR patterns of pure NiO and Ni/MgO catalyst are presented in Figure 1. Pure NiO shows a sharp reduction peak at about 420 °C followed by a small hump. The Ni/MgO catalyst exhibits very small broad peak at 420 °C, which is attributed to relatively free NiO weakly interacting with MgO, and another peak with a maximum at 800 °C, which is attributed to NiO_x strongly interacting with MgO. The reduction degree indicates that only 40.5% NiO is reduced during the TPR process, confirming a strong interaction between NiO and MgO. Studies have established that NiO and MgO are miscible because of their similar crystalline structures and approximate cation radii. They can form solid solution through a mechanism of lattice substitution that leads to a system almost homogeneously mixed at high temperature.[11] Ruckenstein and Hu[9] and Tang *et al.*[11] reported that an ideal solid solution was formed over Ni/MgO catalysts.

Due to the strong interaction between NiO and MgO, nickel can be dispersed uniformly in the support and the segregation of nickel on the surface of support is suppressed during pre-reduction at 700 °C for 3 h.

Pulse Reaction. Sequential pulse experiments ($CH_4 \rightarrow O_2 \rightarrow CH_4$) were performed at 800 °C to investigate the CH_4 dehydrogenation activity and carbon elimination by O_2. In these experiments, five pulses of each gas were injected. The

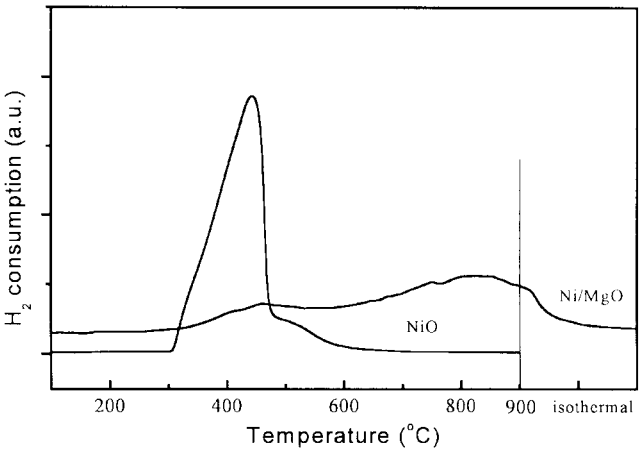

Figure 1. TPR patterns of NiO and Ni/MgO catalysts.

Table 1. Characteristics of Ni/MgO and Ni/$MgAl_2O_4$

Catalyst	Surf. area (m^2/g)	H_2 uptake (μmol/g_{cat})	Dispersion (%)	Surface area of Ni (m^2/g)	Average crystallite dia. (nm)
Ni/MgO	16	8.72	1.68	0.71	58
Ni/$MgAl_2O_4$	18	24.1	2.23	1.96	43

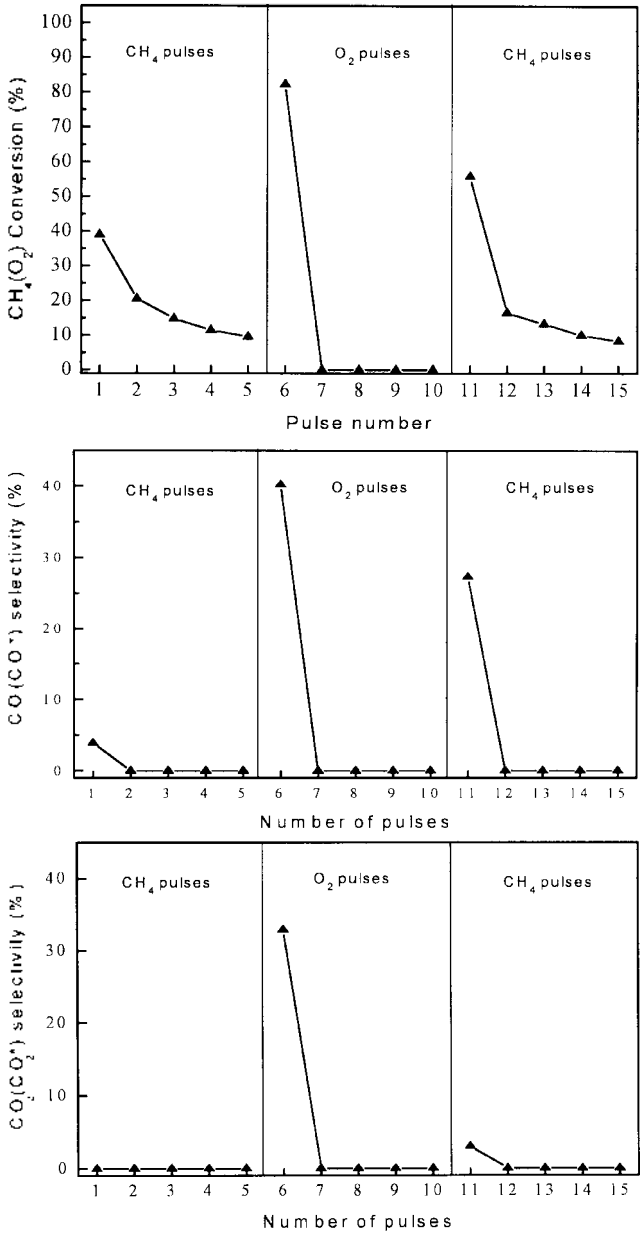

Figure 2. Sequential pulse reaction ($CH_4 \rightarrow O_2 \rightarrow CH_4$) at 800 °C.

blank run in an empty tube and CH_4 pulses over only MgO support did not show detectable CH_4 conversion at 800 °C.

Figure 2 shows CH_4 (O_2) conversion. CO (CO*) and CO_2 (CO_2*) selectivities over Ni/MgO catalyst during three sets of pulses. In the first CH_4 pulse, a large amount of H_2 and a very small amount of CO were detected, implying that CH_4 is effectively decomposed to form carbon species. The CO selectivity for the first pulse was only 3.9% with no CO_2 detection. Since there was no gas-phase oxygen species present in the system after the prereduction at 700 °C for 3 h, the oxygen should originate from the support. However, because reducible oxygen species in the catalyst were very scarce. CH_4 conversion decreased rapidly with increasing CH_4 pulse resulting from coke formation.

To investigate the reaction between surface carbides and O_2, a step switch from CH_4 to O_2 flow was carried out after 5 CH_4 pulses. Huge amounts of CO and CO_2 were produced in the first O_2 pulse, indicating the carbon species could react quickly with surface O species to form CO and CO_2. CO was the main product for the first O_2 pulse. With increasing O_2 pulse number, the amount of CO and CO_2 decreased rapidly due to the elimination of carbon at the first O_2 pulse.

On the basis of the produced carbon and oxygen balances, 0.0419 mmol carbon-containing species were deposited on the catalyst during the first set of methane pulses. The amount of C removed from the catalyst during the second set of oxygen pulses was 0.0416 mmol. and the amount of O adsorbed on the catalyst was 0.0198 mmol. So. carbon species deposited on the catalyst during methane pulses could be removed almost completely by the pulses of oxygen.

To investigate the oxygen species involved in partial oxidation of methane. CH_4 was introduced again after O_2 pulses. Due to the oxygen species still remaining on the catalyst after O_2 pulses. considerable amounts of CO and CO_2 were generated in the first CH_4 pulse. For the first CH_4 pulse in the third set of pulses. CH_4 conversion was higher than that over freshly reduced catalyst in the first set of CH_4 pulses. This indicates that the adsorbed oxygen on the catalyst surface could enhance the conversion of CH_4. The CO selectivity (27.3%) was much higher than CO_2 selectivity (3.0%).

The pulse reactions with the mixture of CH_4/O_2 (2/1) were performed at 600 °C and 800 °C, respectively. The results are shown in Figure 3. During pulsing CH_4/O_2, O_2 was completely converted. Clearly, higher CO selectivity was obtained at higher temperature. This can be explained as follows. One simple explanation is that there was relatively a high amount of O_2 unreacted with CH_4 at lower temperature, resulting in low selectivity to CO. The other reason is that the selectivity to CO is governed mainly by two parallel steps. namely the oxidation of CO(s) to give CO_2 and the desorption of CO(s) to CO(g). Since the activation energy of CO(s) desorption is nearly double that of CO(s) oxidation over Ni, the increase of reaction temperature would favor CO(s) desorption more than CO(s) oxidation. leading to the increase of CO selectivity.[24]

After 10 pulses of CH_4/O_2, pure CH_4 was injected. In the first CH_4 pulse, a considerable amount of CO was formed without CO_2 formation. This indicates that certain oxygen species are present on the catalyst surface after CH_4/O_2 pulses, and these oxygen species favor CO formation. Thus, it can be suggested that the adsorbed oxygen species also play a role as an intermediate in CH_4/O_2 partial oxidation.

Based on the above results. we propose the following mechanism for POM over Ni/MgO catalyst. The dissociative activation of methane on metallic Ni forms surface carbon species and H_2. The carbon species can react with the activated oxygen species on metallic Ni and then form the primary product of CO.

Steady State Activity in POM. POM was carried out at 750 °C. CH_4 to O_2 ratio of 1.875, and 55.200 mL/gh GHSV. The activity in terms of CH_4 conversion. selectivities to H_2 and CO are presented in Figure 4. The catalytic performance

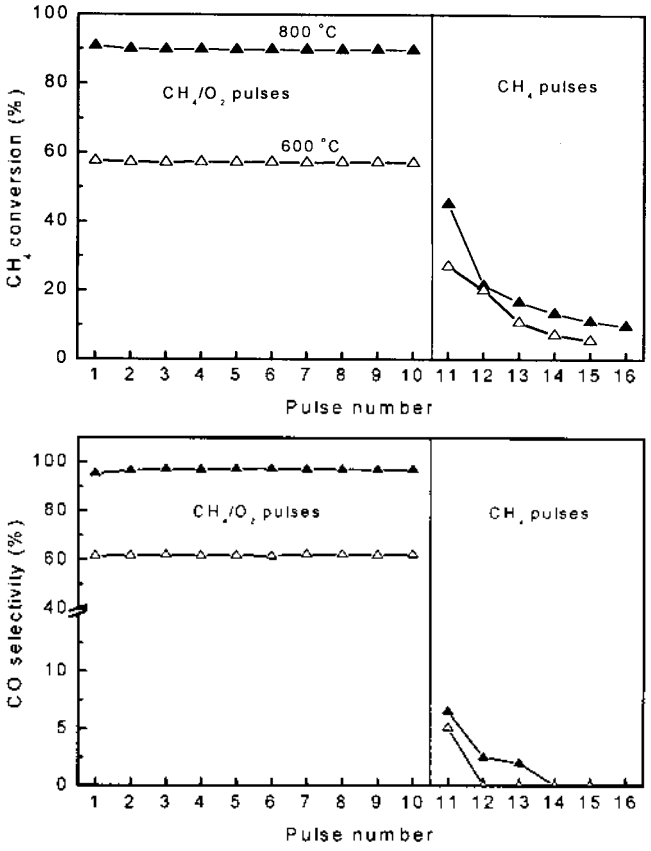

Figure 3. Pulse reaction of CH_4/O_2 (2/1) and CH_4 over Ni/MgO catalyst.

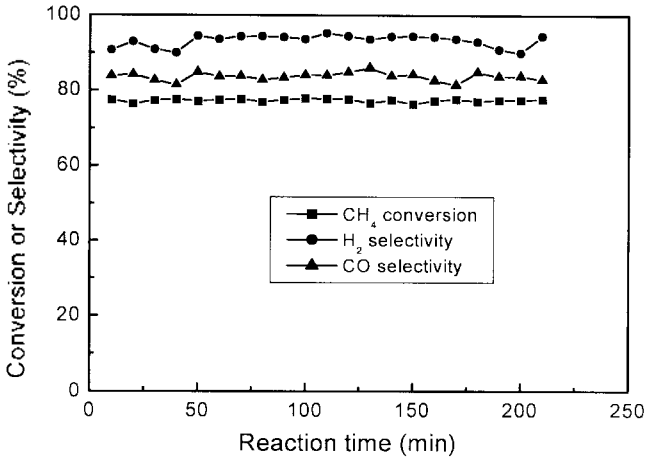

Figure 4. Steady state activities in POM over Ni/MgO catalyst. (Reaction conditions: T = 750 °C, CH_4/O_2 = 1.875, GHSV = 55,200 mL/gh)

was quite stable up to 210 min into the operation. CH_4 conversion was 78% and the selectivities to H_2 and CO were about 95% and 85%, respectively. Consecutive steps of CH_4 dissociation and carbon gasification are believed to have proceeded successfully without further accumulation of carbonaceous intermediates. The highly stable performance of Ni/MgO is due to the strong interaction between NiO and MgO, resulting in the suppression of coke formation. Owing

Table 2. Carbon or oxygen amounts over Ni/MgO during pulse reactions

CH_4 pulse		O_2 pulse	
C deposited (mmol)	C removed (mmol)	C residue (mmol)	O adsorbed (mmol)
0.0419	0.0416	0.0003	0.0198

to the strong interaction between NiO and MgO solid solution, the reduction of NiO was retarded and the reduction temperature window became wide when compared with pure NiO. Thus, relatively small and finely dispersed metallic Ni particles were obtained during reduction treatment. In this case, the metal surface becomes more resistant toward coke formation, because the ensemble size necessary for carbon formation is larger than that for methane reforming.[25] To inhibit carbon formation in a commercial process, sulfur passivation and partial blocking of the active sites are occasionally employed in steam reforming (e.g. SPARG process).[26]

Steady State Activity in SRM. Due to the strong interaction between NiO and MgO, it can be expected that Ni/MgO catalyst would show highly stable activity in SRM, even in stoichiometric feed composition. Thus, SRM was conducted under stoichiometric feed ratio (CH_4/H_2O = 1.0) at 750 °C, with 72,000 mL/gh GHSV over Ni/MgO, and the results are compared with those of $Ni/MgAl_2O_4$, which is widely used in the commercial SRM process. As can be seen in Figure 5, Ni/MgO showed high CH_4 conversion (76%) and there is no obvious deactivation. Namely, the catalyst showed 74% CH_4 conversion after 6 h. Therefore, it was confirmed that both the activity and the stability of Ni/MgO exceeded those of $Ni/MgAl_2O_4$ even in SRM. On the contrary, $Ni/MgAl_2O_4$ deactivated remarkably with time on stream, which was most likely due to the carbon formation. CH_4 conversion was 61% initially, but it decreased to 47% after 6 h. Yamazaki *et al.*[27] reported similar results, saying

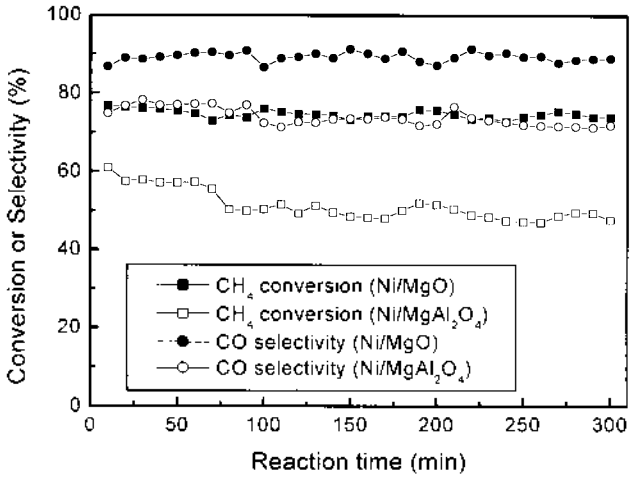

Figure 5. Steady state activities in SRM over Ni/MgO and $Ni/MgAl_2O_4$ catalysts. (Reaction conditions: T = 750 °C, H_2O/CH_4 = 1.0, GHSV = 72,000 mL/gh)

Table 3. CH_4 conversion, CO selectivity, H_2/CO ratio, and H_2/CO_x ratio depending on O_2/CH_4 ratio over Ni/MgO in oxy-steam reforming of methane

O_2/CH_4	0	0.1	0.2	0.3	0.4	0.5
X_{CH4}	74.6	79.3	83.0	85.3	88.4	91.5
S_{CO}	89.4	83.5	78.5	72.6	64.2	54.6
H_2/CO	3.3	3.3	3.3	3.3	3.3	3.3
H_2/CO_x	3.0	2.8	2.6	2.4	2.2	2.1

(Reaction condition: H_2O/CH_4 = 1.0, catalyst = 50 mg. CH_4 = 30 mL/min, T = 750 °C)

that under the condition of low steam/carbon ratio (H_2O/CH_4 = 1.0) commercial reforming catalyst (Ni/Al_2O_3-MgO) is deactivated due to the carbon formation.

Steady State Activity in OSRM. Combined endothermic steam and exothermic oxy-reforming could be carried out simultaneously in an adiabatic reactor without supply of heat. Also, explosion dangers in POM could be eliminated due to the steam introduction and excess steam could be reduced with O_2 supply. Because of these advantages, Ni/MgO catalyst was also examined in OSRM under a different O_2/CH_4 ratio at 750 °C. CH_4 conversion, CO selectivity, H_2/CO ratio, and H_2/CO_x ratio depending on the O_2/CH_4 ratio are summarized in Table 3. CH_4 conversion was proportional to the O_2/CH_4 ratio. CH_4 conversion increased from 74.6% to 91.5% with the increase in O_2/CH_4 ratio from 0 to 0.5. But, CO selectivity decreased from 89.4% to 54.6% due to the water gas shift (WGS) reaction. H_2/CO ratio was kept at 3.3 without regard to the O_2/CH_4 ratio. This strongly indicates that WGS becomes considerable at high O_2/CH_4 ratio. However, the H_2/CO_x ratio decreased from 3.0 to 2.1 with the increase in the O_2/CH_4 ratio from 0 to 0.5. This is mainly due to the fact that SRM is dominant without O_2, whereas POM becomes dominant with the increase in the O_2 feed ratio. Studies have confirmed that H_2/CO_x is 3.0 in stoichiometric feed in SRM and H_2/CO_x is 2.0 in stoichiometric feed in POM. According to the above results, it was confirmed that OSRM could be carried out efficiently over Ni/MgO with the enhanced CH_4 conversion of 91.5%. Yamazaki *et al.*[27] obtained 90% CH_4 conversion over 3 mol% Ni/MgO at 850 °C and 20.000 h^{-1}. Thus, it was also confirmed that more than 90% CH_4 conversion could be achieved in OSRM at 750 °C, which is 100 °C lower than that in SRM with corresponding CH_4 conversion.

Conclusions

Nickel is dispersed uniformly over MgO support due to the strong interaction between NiO and MgO. The dissociative activation of methane on metallic Ni forms surface carbon species and H_2. The carbon species react with the oxygen species originating from O_2 activation on metallic Ni and then form the primary product of CO. Ni/MgO shows high activity and stability in POM, SRM, and OSRM, strongly suggesting that it is a good catalyst candidate in the various modes of methane reforming reactions.

References

1. Wang, J. X.; Lunsford, J. H. *J. Phys. Chem.* **1986**, *90*, 5883.
2. Hutchings, G. J.; Scurell, M. S.; Woodhouse, J. R. *Chem. Soc. Rev.* **1989**, *18*, 25.
3. Pitchai, R.; Klier, K. *Catal. Rev.* **1986**, *28*, 13.
4. Rostrup-Nielsen, J. R. In *Catalytic Steam Reforming Catalysis, Science & Technology*; Anderson, J. R., Boudart, M., Eds.; Springer: Berlin, 1984; vol. 5.
5. Ashcroft, A. T.; Cheetham, A. K.; Foord, J. S.; Green, M. L. H.; Grey, C. P.; Murrell, A. J.; Vernon, P. D. F. *Nature* **1990**, *344*, 319.
6. Choudhary, V. R.; Mamman, A. S.; Sansare, D. *Angew. Chem. Int. Ed.* **1992**, *31*, 1189.
7. Peña, M. A.; Gómez, J. P.; Fierro, J. L. G. *Appl. Catal. A* **1996**, *144*, 7.
8. Choudhary, V. R.; Uphade, B. S.; Mamman, A. S. *J. Catal.* **1996**, *172*, 281.
9. Ruckenstein, E.; Hu, Y. H. *Appl. Catal. A* **1999**, *183*, 85.
10. Diskin, A. M.; Cunningham, R. H.; Ormerod, R. M. *Catal. Today* **1998**, *46*, 147.
11. Tang, S.; Lin, J.; Tan, K. L. *Catal. Lett.* **1998**, *51*, 169.
12. Hickman, D. A.; Schmidt, L. D. *Science* **1993**, *259*, 343.
13. Jones, R. H.; Aschroft, A. T.; Waller, D.; Cheetham, A. K.; Thomas, J. M. *Catal. Lett.* **1991**, *8*, 169.
14. Schmidt, L. D.; Hichman, D. A. *J. Catal.* **1992**, *138*, 267.
15. Tornianan, P. M.; Chu, X.; Schmidt, L. D. *J. Catal.* **1994**, *146*, 1.
16. Ashcroft, A. T.; Cheetham, A. K.; Green, M. L. H.; Vernon, P. D. F. *Nature* **1991**, *352*, 225.
17. Choudhary, V. R.; Rajput, A. M.; Prabhakar, B. *Angew. Chem. Int. Ed.* **1994**, *33*, 2104.
18. Hegarty, M. E. S.; O'Connor, A. M.; Ross, J. R. H. *Catal. Today* **1998**, *42*, 225.
19. Choudhary, V. R.; Rajput, A. M.; Prabhakar, B. *Catal. Lett.* **1995**, *32*, 391.
20. Roh, H.-S.; Jun, K.-W.; Dong, W.-S.; Park, S.-E.; Baek, Y.-S. *Catal. Lett.* **2001**, *74*, 31.
21. Roh, H.-S; Dong, W.-S.; Jun, K.-W.; Park, S.-E. *Chem. Lett.* **2001**, 88.
22. Chang, J.-S.; Park, S.-E.; Chon, H. *Appl. Catal. A* **1996**, *145*, 111.
23. Bartholomew, C. H.; Pannell, R. B. *J. Catal.* **1980**, *65*, 390.
24. Au, C. T.; Wang, H. Y.; Wan, H. L. *J. Catal.* **1996**, *158*, 343.
25. Rostrup-Nielsen, J. R. *Stud. Surf. Sci. Catal.* **1991**, *68*, 85.
26. Udengaard, N. R.; Hansen, J.-H. B.; Hanson, D. C.; Stal, J. A. *Oil Gas J.* **1992**, *90*, 62.
27. Yamazaki, O.; Tomishige, K.; Fujimoto, K. *Appl. Catal. A* **1996**, *136*, 49.